Icarus **156**, 202–210 (2002)
doi:10.1006/icar.2001.6775, available online at http://www.idealibrary.com on IDEAL®

# 10 Hygiea: ISO Infrared Observations[1]

M. A. Barucci

*LESIA, Observatoire de Paris, France*
E-mail: antonella.barucci@obspm.fr

E. Dotto

*INAF, Osservatorio Astronomico di Torino, Italy*

J. R. Brucato

*Osservatorio Astronomico di Capodimonte, Italy*

T. G. Müller

*ISO Data Centre, Astrophysics Division, Space Science Department of ESA, Villafranca, Spain*

P. Morris

*IPAC, Caltech, Pasadena, California*

A. Doressoundiram

*LESIA, Observatoire de Paris, France*

M. Fulchignoni

*LESIA, Observatoire de Paris, France; and Université de Paris VII, France*

M. C. De Sanctis

*IAS, CNR, Rome, Italy*

T. Owen

*University of Hawaii, Honolulu, Hawaii*

J. Crovisier

*LESIA, Observatoire de Paris, France*

A. Le Bras

*LESIA, Observatoire de Paris, France; and IAS, Orsay, France*

and

L. Colangeli and V. Mennella

*Osservatorio Astronomico di Capodimonte, Italy*

Received May 20, 2001; revised August 13, 2001

**Observations of emissivity features of 10 Hygiea have been made for the first time in the relatively unexplored thermal-infrared wavelength region with the ISO (Infrared Space Observatory) satellite. Spectrophotomer (PHT-S) and short wavelength spectrometer (SWS) spectra of 10 Hygiea, obtained at 5.8–11.6 and 7–45 $\mu$m, respectively, are presented. In order to remove the thermal emission continuum, an advanced thermo–physical model has been applied to the observational data. To better interpret the spectral features above the thermal emission continuum, we compared the ISO observations with laboratory spectra available in the literature.**

[1] Based on observations with ISO, an ESA (European Space Agency) project with instruments founded by ESA Member States (especially the PI countries: France, Germany, the Netherlands, and the United Kingdom) with the participation of ISAS and NASA.



0019-1035/02 $35.00

**Several laboratory experiments on minerals and meteorites have been performed to complete the analysis and to study the spectral behavior at various grain sizes. A possible spectral similarity with CO carbonaceous chondrites at small grain size is demonstrated.** 

*Key Words:* **asteroids; 10 Hygiea; infrared observations; spectroscopy; ISO.**

## 1. INTRODUCTION

Observations of the asteroid 10 Hygiea have been performed for the first time in the wavelength range 5.8–45 $\mu$m by the Infrared Space Observatory (ISO), an ESA project launched on November 1995 and operative until April 1998 (Kessler *et al.* 1996). These observations allowed us to investigate the surface composition of this object, which belongs to the C taxonomic type (Barucci *et al.* 1987, Tholen 1989, Tedesco *et al.* 1989, Bus 1999). The C class contains primitive dark objects whose visible to near-IR wavelength characteristics are similar to those of carbonaceous chondrite meteorites (Chapman and Salisbury 1973, Gaffey *et al.* 1993, Hiroi and Vilas 1995). These asteroids are very common, especially in the outer part of the main belt, and their investigation should yield information about the early chemical and physical processes operating in this portion of the Solar Nebula. Lebofsky (1980) and Jones *et al.* (1990) presented the first evidence of the presence of aqueous alteration products on C-type asteroids. Aqueous alteration products are linked with the strong absorption feature at about 3 $\mu$m due to water of hydration. Aqueous alteration is a low temperature chemical alteration of materials by liquid water. This could indicate the presence of water ice originally in these asteroid types which were heated sufficiently to melt, producing water responsible for this chemical alteration. Selective induction heating may have produced aqueous alteration at the surface, resulting in the carbonaceous chondrite parent bodies. Vilas *et al.* (1994), on the basis of visible observations, proposed that a particular region of the outer main belt (between 2.6 and 3.5 AU) seems to be characterized by objects which have undergone some kind of aqueous alteration process. Barucci *et al.* (1998) confirmed the existence of this zone and found that 70% of C-class asteroids located there show evidence of aqueous alteration.

Asteroid 10 Hygiea, named in honor of the Greek goddess of health, daugther of Aesculapius, was discovered in 1849 by A. de Gasparis in Naples. It is the fourth largest asteroid, after 1 Ceres, 2 Pallas, and 4 Vesta, with an IRAS diameter of 407 km and an albedo $pv = 0.07$ (Tedesco *et al.* 1992). Hygiea rotates around its principal axis in a retrograde sense with a period of $27.63 \pm 0.02$ h (Michalowski *et al.* 1991, Erikson and Magnusson 1993, and López-González and Rodríguez 2000). On the basis of Speckle interferometry, Ragazzoni *et al.* (2000) found a shape with an average diameter of $444 \pm 35$ km and a semimajor axis ratio $a/b = 1.11$. Storrs *et al.* (1999) observed Hygiea with the Hubble Space Telescope (HST), obtaining only marginal resolution of the object, and they did not detect any companion down to a limit seven magnitudes fainter than the primary asteroid. Aqueous alteration products have been detected on Hygiea's surface by Jones *et al.* (1990) and Vilas (1994) on the basis of 3.0-$\mu$m and 0.7-$\mu$m absorption features. Other observations in the visible region were performed at different epochs, but the 0.7-$\mu$m absorption feature (Bus 1999, Fornasier *et al.* 1999) was not detected. These results may imply compositional variation on the surface. Tentative characterization of the surface composition has been made by Lebofsky *et al.* (1985), who studied the thermal properties of Hygiea (observations at 2.2, 10.6, 21, 370 and 770 $\mu$m) and concluded that Hygiea is a dusty object, whose surface could be dustier and more mature than the surface of the Moon. Johnston *et al.* (1989), on the basis of microwave observations of Hygiea at 2 and 6 cm, derived a regolith layer of depth greater than 8 cm. Rivkin (1997), looking for variation in the 3-$\mu$m spectral region, found some latitudinal variations that were due to possible excavations of interior layers, but he found no clear evidence of variation with the rotation. The latter was found, however, by Mothé-Diniz *et al.* (2001) on the basis of visible data only. Comparing reflectance spectra of a few selected C, G, B, and F asteroids with spectra of a few tens of carbonaceous chondrites, Hiroi *et al.* (1996) found a good match between the 0.3–3.6-$\mu$m spectrum of Hygiea and an unusual CI/CM meteorite (Y-82162).

## 2. OBSERVATIONS

The Hygiea observations were performed with ISO using the imaging photopolarimeter ISOPHOT (Lemke *et al.* 1996) and the short wavelength spectrometer (SWS) (de Graauw *et al.* 1996). In particular, we used the subsystem spectroPhoTomer (PHT–S), which consists of two low-resolution grating spectrometers which cover the wavelength range 2.5–5 $\mu$m (PHT–SS) and 6–12 $\mu$m (PHT–SL). PHT–SS and PHT–SL have a common square entrance aperture of $24 \times 24$ arcsec. The resolution $\lambda/\Delta\lambda$ is about 85 for PHT–SS and about 95 for PHT–SL.

The PHT observations were performed in staring mode with a default of 32 sec dark exposure at the beginning of the measurement. ISOPHOT interactive analysis (PIA[2]) V7.3.3 was used for the standard data reduction up to signal level, including linear ramp fitting, deglitching on ramp and signal level, and orbit-dependent dark signal subtraction (Gabriel *et al.* 1997). The calibration of the derived signal was done with the *dynamic calibration* method (Laureijs *et al.* 2001) using two calibration standards for each detector pixel, combined by weighting the ratios between the target and calibrator signals.

The SWS was employed in a mode designed to yield maximum spectral resolution (astronomical observing template 6; de Graauw *et al.* 1996) with its grating sections, $\lambda/\Delta\lambda = 1500$–3200. The two grating sections separately cover 2.38–12.0 and 12.0–45.2 $\mu$m and are independently wavelength and flux

[2] PIA is a joint development by the ESA Astrophysics Division and the ISOPHOT consortium.

**TABLE I**
**Aspect Data of the Asteroid 10 Hygiea**

| Detector | Observation date | Start time (UT) | Integration time (sec) | $\Delta$ (AU) | $r$ (AU) | $\alpha$ (deg) |
|---|---|---|---|---|---|---|
| PHT–S | 06/12/96 | 17:59:33 | 172 | 2.94 | 3.45 | 15.1 |
| SWS | 16/09/97 | 03:48:04 | 11290 | 3.36 | 3.51 | 16.7 |

calibrated with internal sources and a grid of celestial standards (Kester *et al*. 1998, and Morris 1999).

Reductions of the SWS observations were performed in the OSIA (observers SWS interactive analysis package) environment, using software and calibration files compatible with version 6.0 or higher of the ESA data pipeline (Leech *et al*. 2001). Some processing steps were performed interactively, such as broadband correction of fluxes for spacecraft tracking effects. This step requires the use of the spacecraft pointing history and detailed knowledge of the SWS spatial responsivities in its $14'' \times 20''$ to $27'' \times 33''$ apertures. Inspection of dark currents and scan data, correction of erratic behavior, from each of the 12 detectors employed in each of the 4 arrays (2 per grating section, 48 detectors total), and coaddition of the final, fully calibrated output were also performed interactively.

The SWS observations were planned to give optimum signal/noise (S/N) ratios in the heretofore unexplored thermal regime of Hygiea's spectral energy distribution. The 2.4–7 $\mu$m reflected-thermal transition spectrum suffers from low gain settings and short integration times and yields S/N ratios $<$10. We exclude these data, because the reflected-thermal transition range is not usually included in thermal modelling programs.

Table I lists the observational parameters of Hygiea. Note that the duration of the SWS observations is substantially longer than the PHT–S observations, occuring over $\sim$10% of Hygiea's rotation period.

In Figs. 1 and 2 show the resulting low-resolution spectrum in the range 5.8–11.6 $\mu$m and the high-resolution spectrum between 7 and 45 $\mu$m, respectively. The absolute uncertainty between SWS and PHT–S is less than 5%. The good match of the spectra obtained with the two different instruments (see the top of Fig. 5) strengthens our confidence regarding the good quality of ISO data and calibration in this wavelength range. The accuracy of band 4 (30–45 $\mu$m) of the SWS is not very good: in Volume VI of the ISO handbook (Leech *et al*. 2000) it was reported that the shape of the current band 4 relative spectral response function (RSRF) has an inaccuracy of about 10%. The features present beyond 30 $\mu$m in the Hygiea spectrum are within the relative broadband uncertainty and for this reason we do not consider this part of the spectrum in our analysis.

The emissivity of asteroids beyond 5 $\mu$m is dominated by radiation thermally emitted from their surfaces. A black-body fit was applied to the infrared data and a black-body temperature $T_{BB} = 200$ K was determined. The subsolar temperature

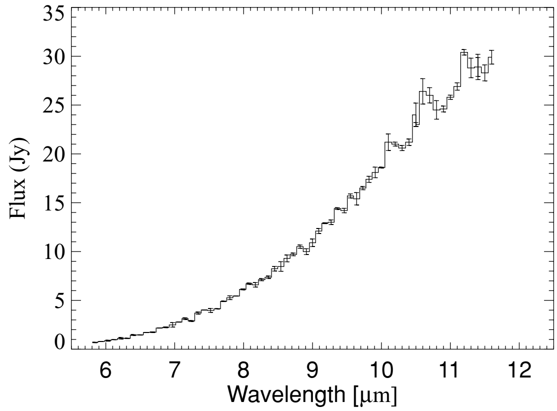


**FIG. 1.** PHT–S spectrum of 10 Hygiea obtained in the range 5.8–11.6 $\mu$m. The relative error bars are reported.

of Hygiea has been computed by applying the standard thermal model (Lebofsky and Spencer 1989),

$$T_{SS} = \left[\frac{(1-A)S}{\eta\varepsilon\sigma}\right]^{1/4} \quad \text{and} \quad T(\Omega) = T_{SS}\cos^{1/4}(\Omega), \quad (1)$$

where $\Omega$ is the solar zenith angle, $A$ is the bolometric Bond albedo, $S$ is the solar flux at the distance of the asteroid, $\eta$ (infrared beaming) is an empirical factor adjusted so that the model matches the integrated flux of the object at a given wavelength, $\varepsilon$ is the wavelength-independent emissivity, and $\sigma$ is the Stefan–Boltzmann constant. The resulting value of the subsolar temperature is $T_{SS} = 230 \pm 5$ K.

In order to investigate the features of the infrared spectra in a detailed way, we applied the advanced thermo–physical model (TPM) developed by Lagerros (1996, 1997, 1998), refined by

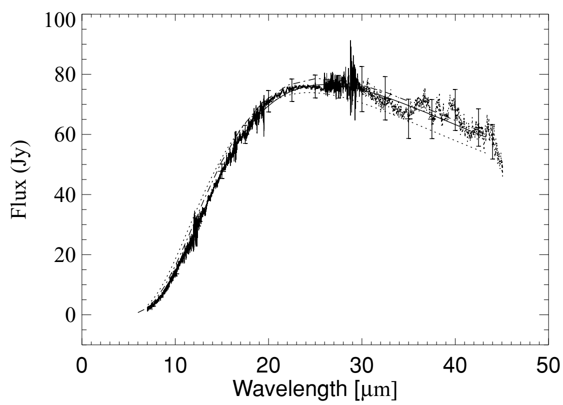


**FIG. 2.** SWS spectrum of 10 Hygiea obtained up to 45 $\mu$m with the relative error bars. Since the features present beyond 30 $\mu$m are within the relative broadband uncertainty, a dashed line is given for the final part of the spectrum. The best-fitting black-body continuum (continuous line), the STM continuum (dotted line), and the TPM continuum (dashed–dotted line) are overlapped with the observations.

**TABLE II**
**TPM Input Parameters of 10 Hygiea**

| $H$ (mag) | $G$ | $p_v$ | Diam (km) | $a/b$ | $b/c$ | $\lambda_p$ ($^o$) | $\beta_p$ ($^o$) | $P_{sid}$ (days) | $\gamma_o$ ($^o$) | $JD_o$ |
|---|---|---|---|---|---|---|---|---|---|---|
| 5.44 | 0.22 | 0.066 | 429.9 | 1.29 | 1.18 | 294 | –35 | 1.150974 | 105 | 2444239.5 |

Müller and Lagerros (1998), and already used on asteroid data by Müller *et al.* (1999) and Dotto *et al.* (2000). TPM calculates the energy balance between absorbed solar radiation, thermal emission, and heat conduction into the surface material, considering the object as a rotating ellipsoid. This TPM includes a beaming model (Lagerros 1996), thermal inertia, and a wavelength-dependent emissivity (Müller and Lagerros 1998). In the case of Hygiea, default values for the beaming ($\varrho = 0.7$ and $f = 0.6$), the thermal inertia ($\Gamma = 15\ J\ \mathrm{m}^{-2}\ \mathrm{s}^{-0.5}\ \mathrm{K}^{-1}$), and the wavelength-dependent emissivity have been used (Müller and Lagerros 1998, Müller *et al.* 1999). Table II reports all the TPM input parameters (absolute magnitude $H$, slope parameter $G$, geometric albedo $p_v$, diameter, semimajor axes $a/b$ and $b/c$, pole coordinates, sidereal period, absolute rotational phase, and zero point time). The slope parameter $G$ and the geometric albedo $p_v$ values have been taken from Müller and Lagerros (1998). Shape, sidereal period, and spin vector are known from photometric observations, and the absolute size has been derived by means of the radiometric method (Müller and Lagerros 1998). Converting the measured SWS spectrum to brightness temperature, we obtain $T_{TPM} = 196 \pm 2$ K. The emissivity spectrum of the asteroid (Figs. 3a and 3b and Fig. 4, on the top) was obtained as a ratio of the ISO spectrum to the thermo–physical model.

## 3. LABORATORY SPECTRA AND RESULTS

To interpret Hygiea's surface composition we considered databases of laboratory spectra of minerals and/or meteorites[3] (Salisbury *et al.* 1991a,b, Carmichael 1989). Moreover, several minerals have been selected as possible candidates to be present on the surface of the C-type asteroids (Gaffey *et al.* 1993, Hiroi *et al.* 1995), and laboratory spectra of these have been recorded (see Table III and Figs. 3a and 3b). Most of the C-type asteroids, in fact, have revealed the presence of spectral features of hydrated minerals, such as phyllosilicates, or of olivines and pyroxenes. Aqueous alteration of minerals is an active process which could have taken place on the C-type asteroids and could be responsible for the formation of, e.g., iron oxides. None of the analyzed mineral spectra matches the Hygiea spectrum. Many attempts have been made to combine (by intimate and geographical mixing models) these different components while maintaining consistency with the hypothesized composition, and the quality of the numerous matches is always very poor.

We compared our measurements of Hygiea to all the different kinds of meteorites available on the ASTER spectral library[3] (spectra of 60 different meteorites). The most consistent analogy is with spectra of the carbonaceous chondrite meteorites. This confirms previous work in which C-type asteroids were associated with this type of meteorite.

As suggested by Le Bertre and Zellner (1980), the asteroid spectra are dominated by effects due to the presence of fine particles on their surfaces. Thus it is important to analyze the optical properties of particulate samples with various grain sizes in the laboratory. To this end, new laboratory experiments on four different carbonaceous chondrites (CI, CO, CR, and CM; see Table III) have been performed to obtain infrared spectra up to 45 $\mu$m at various grain sizes not yet available in the literature (Fig. 4). Several size ranges were selected, from a few microns up to 100–200 microns.

The Capodimonte Observatory Bruker IFS66v interferometer was used to obtain laboratory spectra. Diffuse reflectance measurements at a resolution of 2 $\mathrm{cm}^{-1}$ have been obtained by equipping the instrument with a Graseby Specac Mod. Selector accessory. Spectral measurements have been performed at low pressure (1 mbar) to prevent changes of the environmental conditions (e.g., atmospheric water vapor and carbon dioxide abundance) during measurements, which could affect the spectral results. The optical configuration used was biconical, i.e., the infrared beam was focused onto the sample by means of an ellipsoidal mirror and collected by another ellipsoidal mirror, at 90° from the incident beam. This configuration has the advantage of very high collection efficiency and it is appropriate for accurate determination of the reflectance profile by measuring diffuse reflectance at 90° with respect to the principal plane. Such an experimental set-up prevents possible distortion of the Christiansen feature, due to preferential forward scattering, which can occur when biconical reflectance is measured in the principal plane (e.g., Salisbury *et al.* 1991a).

The diffuse reflectance of the particulates $R$ is obtained as the ratio between the diffuse reflectance of the sample $R_s$ and of the reference $R_r$ ($R = R_s/R_r$). Our measurements were performed using finely ground pure CsI powder as a reference.

Even if the Hygiea spectrum at wavelengths >5 $\mu$m refers to the emittance of the body (the power thermally emitted by the surface), usually diffuse reflectance measurements can be used for comparison. To enable the data obtained in the laboratory to be compared with the ISO spectra, the emissivity $E$ of the particulate samples was derived via Kirchhoff's law from the diffuse reflectance, $E = 1 - R$, while Hygiea's emissivity was calculated as a ratio of the ISO spectrum to the thermo–physical model. For the meteorites, we report the emissivity of a bulk sample of Murchison, and of different grain size ranges for samples of Ornans, Renazzo, and Orgueil. The emissivity behavior is drastically grain-size dependent for the same meteorite. In

[3] ASTER spectral library at speclib.jpl.nasa.gov and the Optical Data of Cosmic Dust Analogues at www.astro.uni-jena.de/Group/Subgroups/Labor/Labor/odata.html.

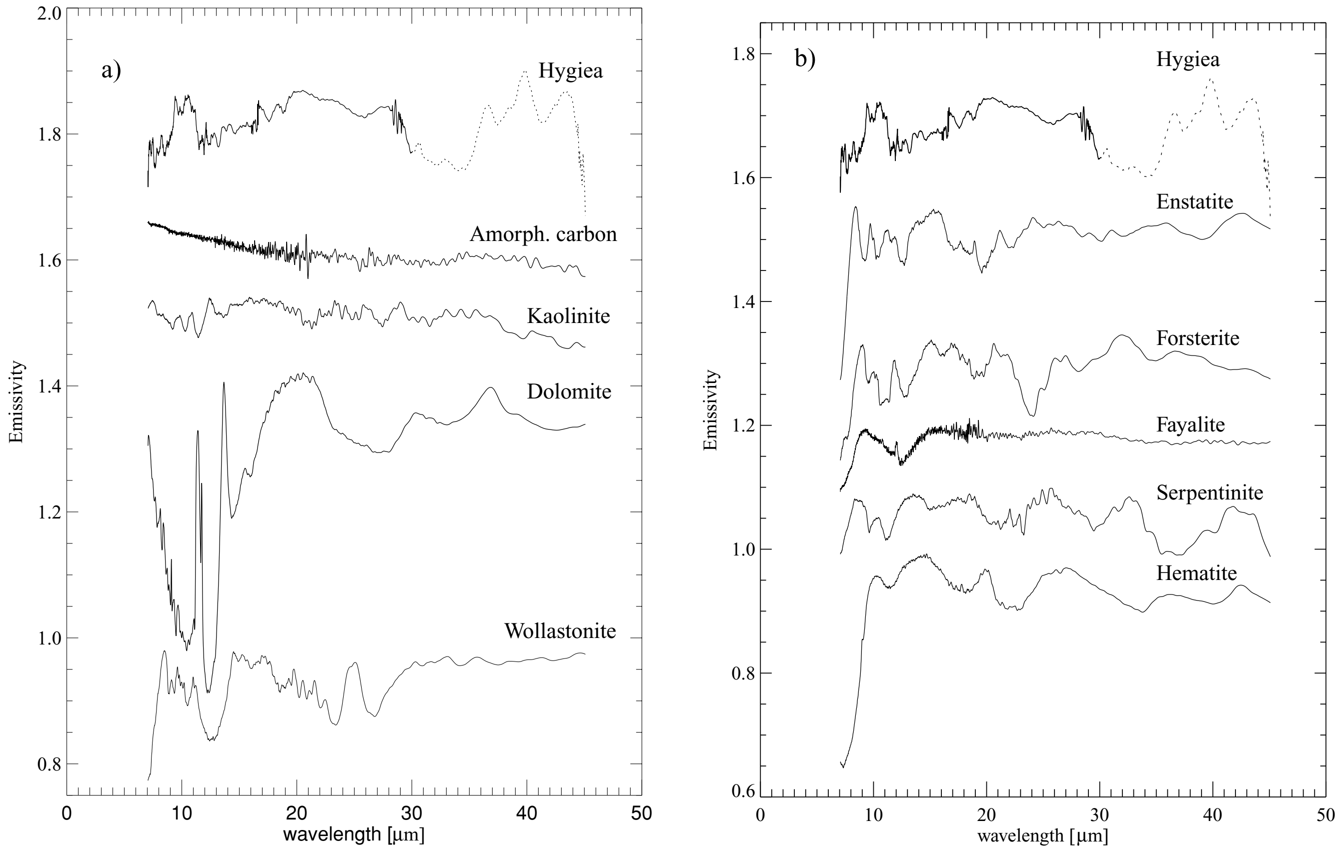


**FIG. 3.** Emissivity of mineral samples obtained by experiments performed at the Capodimonte Observatory. They are vertically offset for clarity. On the top, we give the Hygiea spectrum transformed into emissivity. Since the features present in the ISO spectrum beyond 30 $\mu$m are within the relative broadband uncertainty, a dashed line is used for the final part of the spectrum.

particular, inside the same meteorite the Christiansen peak strength changes with the grain size. Many authors analyzed and discussed this effect in detail (Salisbury *et al.* 1991a,b, Salisbury 1993).

The main features observable in the spectra of selected minerals (Figs. 3a and b) and of carbonaceous chondrite meteorites (Fig. 4), which are diagnostic of the mineralogical and petrologic assembly of the analyzed materials, can be classified into three classes: Christiansen, reststrahlen, and transparency features (a detailed description of these features is given in Salisbury 1993).

**TABLE III**
**Carbonaceous Chondrite Meteorites and Minerals Analyzed in the Laboratory**

| | |
|---|---|
| CI: | Orgueil (0–50; 50–100; 100–200; >200 $\mu$m) |
| CO: | Ornans (0–20; 20–50; 50–100; >100 $\mu$m) |
| CR: | Renazzo (0–20; 20–50; 50–100; >100 $\mu$m) |
| CM: | Murchison (bulk) |
| Carbonate: | Dolomite (0–50 $\mu$m) |
| Phyllosilicate: | Kaolinite; Serpentinite (0–50 $\mu$m) |
| Amorphous Carbon Oxide: | Hematite (0–50 $\mu$m) |
| Olivine: | Fayalite (0–50 $\mu$m) |
| | Forsterite (0–50 $\mu$m) |
| Single-chain pyroxene: | Enstatite (0–50 $\mu$m) |
| Single-chain nonpyroxene: | Wollastonite (0–50 $\mu$m) |

*Christiansen feature*. Rapid changes in the refractive index are responsible for an anomalous dispersion that makes the particulate sample transparent. This phenomenon produces the appearance of the Christiansen feature at shorter wavelengths with respect to the reststrahlen features. The Christiansen feature, which is directly related to the mineralogy and the grain size, appears in the emissivity spectra of Fig. 4, as a peak between 8 and 9.4 $\mu$m. To reveal the Christiansen peak more clearly, the spectra up to 11.6 $\mu$m are shown in Fig. 5.

*Reststrahlen features*. These features are due to the vibrational modes of molecular complexes. The absorption coefficient at resonance wavelengths is very strong, producing the most intense bands in the infrared spectrum by surface scattering. For smaller grain sizes, the main reststrahlen features decrease their spectral contrast. A plateau is visible between 9 and 12 $\mu$m in the spectra shown in Fig. 4, in particular in the Ornans meteorite.

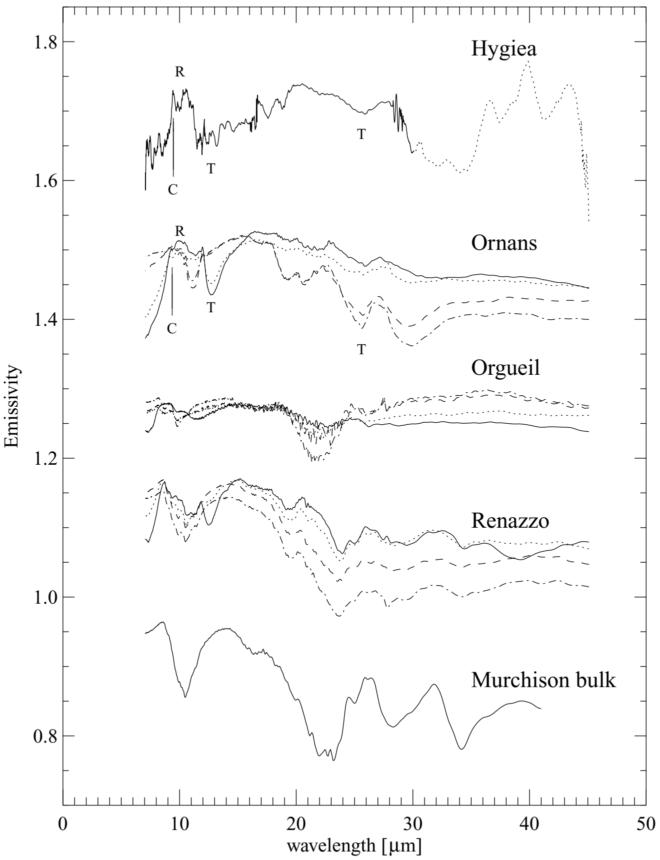


**FIG. 4.** Emissivity of carbonaceous chondite meteorite samples obtained by experiments performed at the Capodimonte Observatory. For each meteorite, different grain sizes are reported. In particular, we considered for Ornans and Renazzo the grain dimensions 0–20 $\mu$m (continuous lines), 20–50 $\mu$m (dotted lines), 50–100 $\mu$m (dashed lines), and >100 $\mu$m (dashed–dotted lines); while for Orgueil we considered 0–50 $\mu$m (continuous line), 50–100 $\mu$m (dotted line), 100–200 $\mu$m (dashed line), and >200 $\mu$m (dashed–dotted line). They are vertically offset for clarity. On the top, the Hygiea spectrum transformed into emissivity is given. Since the features present beyond 30 $\mu$m are within the relative broadband uncertainty, a dashed line represents the final part of the spectrum.

*Transparency features*. In the spectral region where the absorption coefficient decreases, grains become more transparent. Usually, this occurs at 11–13 $\mu$m between main reststrahlen bands and at longer wavelengths (>30 $\mu$m) where the absorption coefficient decreases (Mennella *et al*. 1998). If the grain size is small, volume scattering occurs and transparency features are observable due to a loss of photons crossing many grains. As shown in Fig. 4, the structure at about 11–13 $\mu$m is more evident in the spectrum of all the considered powdered meteorites for smaller grain dimensions. The feature at about 26 $\mu$m, on the contrary, is more evident for bigger grain sizes, except for Orgueil.

## 4. DISCUSSION

The top of Fig. 5 shows the PHT–S and SWS emissivity of 10 Hygiea obtained by dividing the observed PHT–S and SWS fluxes by the TPM expected fluxes. This plot facilitates comparison of observations taken at different epochs (times) to search for spectral features above the thermal emission continuum. The flux levels and the structures in the two spectra are the same, within the uncertainties. The interpretation of the continuum of reflectance or emissivity of an asteroid surface is difficult and not unique, since asteroid surfaces are composed of mixtures of minerals whose spectral properties are nonlinearly combined. Asteroid spectra are affected not only by the chemical composition of the surfaces, but also by several physical parameters, such as particle size, porosity, packing, and thermal gradients. In this spectral range (5.8–11.6 $\mu$m), the most diagnostic feature is the Christiansen peak. Fig. 5 also shows the emissivity obtained by our laboratory experiments for several carbonaceous chondrite samples at different grain sizes. As shown by Salisbury *et al.* (1991b), the Christiansen feature of carbonaceous chondrites occurs at longer wavelengths than it does for other meteorite types. From the comparison of the Hygiea spectra with the meteorite emissivity, we have found that the feature at about 9.3 $\mu$m of Hygiea seems to be more consistent with the Christiansen peak of Ornans grains in the small size range.

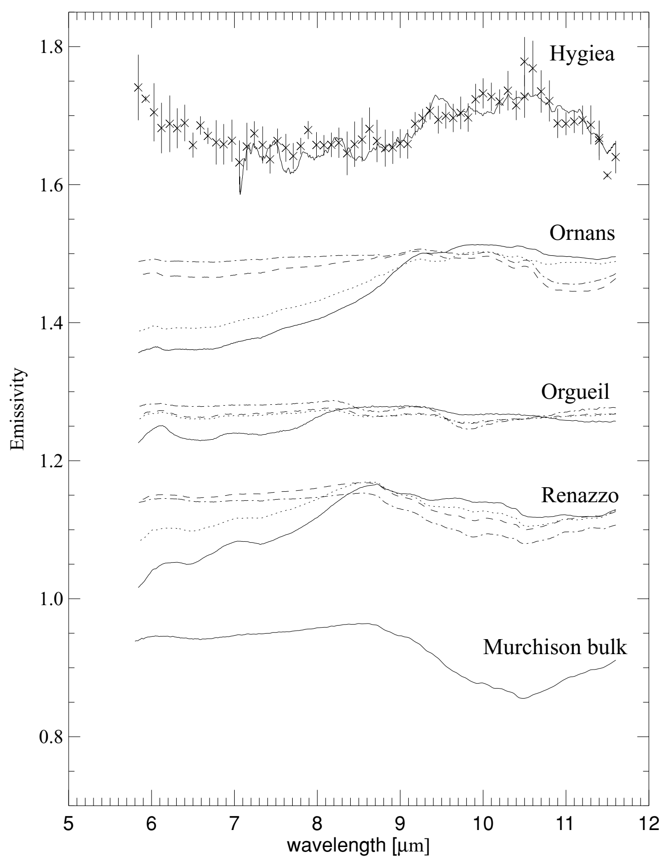


**FIG. 5.** Relative PHT–S (crosses) and SWS (continuous line) observations of Hygiea divided by the TPM expected flux, compared up to 11.6 $\mu$m with the emissivity of the carbonaceous chondrite meteorites obtained by laboratory experiments (see Fig. 4 caption).

From the comparison of Hygiea with the ASTER meteorites, the best agreement has been found with CO meteorite Warrenton (Fig. 6). Ornans and Warrenton represent the greatest similarity with the spectral behavior of Hygiea up to about 27 $\mu$m. The analogy is supported by the comparison of the Christiansen peak at ~9.3 $\mu$m and by the transparency features around 13 $\mu$m and at 26 $\mu$m. For longer wavelengths (see Figs. 3 and 4), we are not able to interpret the features present beyond 30 $\mu$m, in particular those at 35–42 $\mu$m. They are just inside the relative broadband uncertainty of band 4 (30–45 $\mu$m) of SWS, but we report the entire ISO observed spectrum to allow possible future comparison on this spectral region.

Ornans and Warrenton are type 3 carbonaceous meteorite chondrites (CO3). The CO carbonaceous chondrites consist of small condrules and aggregates set in a fine-grained matrix which varies from 30 to 40% by volume. The matrix of these meteorites consists of a heterogeneous mixture of fine-grained iron-rich olivine and hydrated silicates (Sandford 1984). These CO3 meteorites seem to show the presence of aqueous alteration processes (Zolensky and McSween 1988), although the possible products of aqueous alteration within CO chondrites have received limited attention. In fact, although present in these meteorite classes, they are not as pervasive as in the CIs and CMs. This result does not contradict the analogy found by Hiroi *et al.* (1996) of Hygiea with the unusual CI/CM meteorite Y–82162 which implies thermal metamorphism.

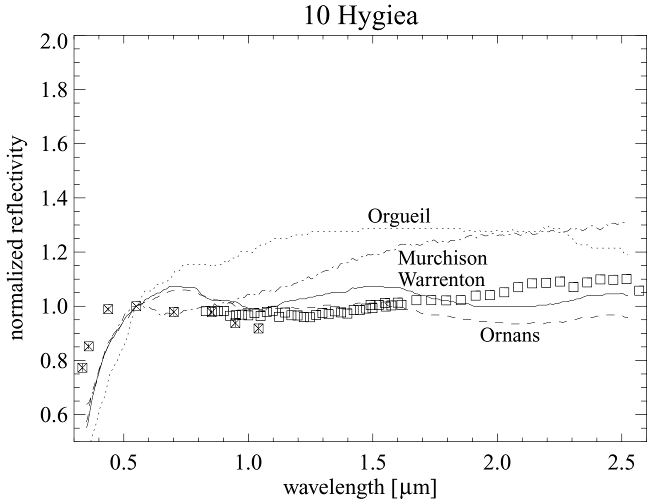


**FIG. 7.** Spectrum of Hygiea in the visible (squares and crosses) and near-infrared (squares) region, observed both by ECAS and the 52-asteroid survey and compared with four different samples of carbonaceous chondrites taken from the Gaffey meteorite collection (Gaffey 1976).

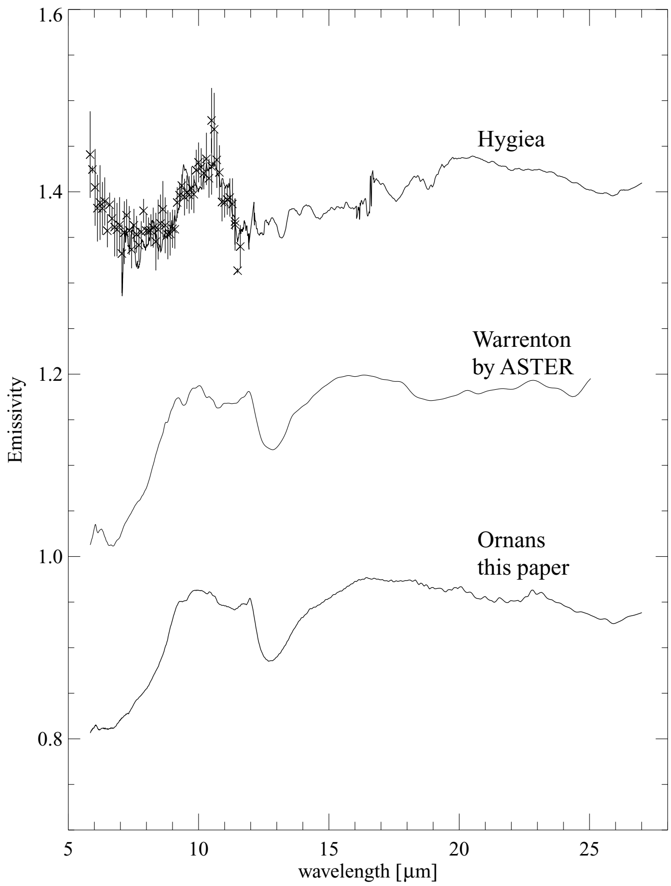


**FIG. 6.** Comparison between PHT–S and SWS emissivity of 10 Hygiea and the laboratory emissivity of Ornans (this paper) and Warrenton (from the ASTER database).

Because of their spectral similarity in the visible and near-infrared regions, C-type asteroids have always been associated with CI and CM meteorites especially due to their matching weak absorption features in the shortest wavelength regions.

We compared the visible and near-IR spectra of Hygiea available in the literature with the Orgueil, Ornans, Warrenton, and Murchison spectra taken from the Gaffey meteorite spectral database (Gaffey 1976) (Fig. 7). Although none of these spectra fits the Hygiea spectrum perfectly, the CO meteorite (Ornans and Warrenton) spectra show a general trend that is closer to the Hygiea spectrum in this region than the CI and CM meteorites.

## 5. CONCLUSIONS

We have presented the first observations of the asteroid 10 Hygiea obtained by ISO in the infrared wavelength region. The standard–thermal model and an advanced thermo–physical model have been applied to the infrared data to model the thermal continuum. To interpret the spectral features above the thermal emission continuum we compared the ISO spectra with laboratory spectra available in the literature.

We also present new laboratory spectra of several minerals and meteorites obtained at wavelengths from 7 to 45 $\mu$m. For the meteorites, the effect of the grain sizes, ranging from $<20$ $\mu$m up to $>200$ $\mu$m is presented.

In summary, our conclusions are:

(1) None of the mineral spectra considered matches the Hygiea spectrum.

(2) The best match in the case of the meteorite spectra is with Ornans and Warrenton meteorites (CO3 carbonaceous chondrites), although the emissivity is strongly grain-size dependent. Optical and near-IR spectra also reveal a better match to CO meteorites than to CI and CM meteorites.

(3) The match to carbonaceous chondrites supports the view that Hygiea is a "primitive" object that has undergone slight thermal alteration and some aqueous alteration. Hygiea is one of the biggest asteroids of the main belt and thus may have supported some initial stage of metamorphism.

## ACKNOWLEDGMENTS

We are indebted to G. Consolmagno (Specola Vaticana, Rome, Italy) and C. Perron (M.N.H.N., Paris, France) for providing the meteorite samples. In particular, we are very grateful to J. Salisbury for his constructive comments and suggestions. We also thank the referees, Beth E. Clark and Alain W. Harris (DLR), for their valuable work in improving this paper. OSIA is a joint development of the SWS consortium; contributing institutes are SRON, MPE, KUL, and the ESA Astrophysics Division.

## REFERENCES

Barucci, M. A., M. T. Capria, A. Coradini, and M. Fulchignoni 1987. Classification of asteroids using G-mode analysis. *Icarus* **72**, 304–324.

Barucci, M. A., A. Doressoundiram, M. Fulchignoni, M. Florczak, M. Lazzarin, C. Angeli, and D. Lazzaro 1998. Search for aqueously altered materials on asteroids. *Icarus* **132**, 388–396.

Bus, B. 1999. *Compositional Structure in the Asteroid Belt: Results of a Spectroscopic Survey.* Ph.D. thesis, Massachusets Institute of Technology, Cambridge, MA.

Carmichael, R. S. 1989. *Practical Handbook of Physical Properties of Rocks and Minerals*. CRC Press, Boca Raton, FL.

Chapman, C. R., and J. W. Salisbury 1973. Comparisons of meteorite and asteroid spectral reflectivities. *Icarus* **19**, 507–522.

de Graauw, T., and 31 colleagues 1996. SWS observations of solid $CO_2$ in molecular clouds. *Astron. Astrophys.* **315**, 49–54.

Dotto, E., and 10 colleagues 2000. ISO results on bright Main Belt asteroids: PHT-S observations. *Astron. Astrophys.* **358**, 1133–1141.

Erikson, A., and P. Magnusson 1993. Pole determinations of asteroids. *Icarus* **103**, 62–66.

Fornasier, S., M. Lazzarin, C. Barbieri, and M. A. Barucci 1999. Spectroscopic comparison of aqueous altered asteroids with CM2 carbonaceous chondites meteorites. *Astron. Astrophys. Supp.* **135**, 65–73.

Gabriel, C., J. A. Acosta–Pulido, I. Heinrichsen, H. Morris, and W.-M. Tai 1997. In *Astronomical Data Analysis Software and Systems*, Vol. VI. (G. Hunt and H. Payne, Eds.), ASP Conference Series 125, p. 108. Astron. Soc. of the Pacific, San Francisco, CA.

Gaffey, M. J. 1976. Spectral reflectance characteristics of the meteorite classes. *J. Geophys. Res.* **81**, 905–920.

Gaffey, M. J., T. H. Burbine, and R. P. Binzel 1993. Asteroid spectroscopy—Progress and perspectives. *Meteoritics* **28**, 161–187.

Hiroi, T., and F. Vilas 1995. Characterization of absorption bands (0.6–0.9 microns) in reflectance spectra of primitive asteroids. *Lunar Planet. Sci.* **26**, 611.

Hiroi, T., C. M. Pieters, M. E. Zolensky, and M. E. Lipschutz 1995. Possible thermal metamorphism on the C asteroids seen from the E3-micrometer hydration band in comparison with heated CI/CM meteorites. *Meteoritics* **30**, 521.

Hiroi, T., M. E. Zolensky, C. M. Pieters, and M. E. Lipschutz 1996. Thermal metamorphism of the C, G, B, and F asteroids seen from the 0.7 $\mu$m, 3 $\mu$m, and UV absorption strengths in comparison with carbonaceous chondrites. *Meteor. Planet. Sci.* **31**, 321–327.

Johnston, K. J., E. J. Lamphear, W. J. Webster, P. D. Lowman, P. K. Seidelmann, G. H. Kaplan, C. M. Wade, and R. W. Hobbs 1989. The microwave spectra of the asteroids Pallas, Vesta, and Hygiea. *Astron. J.* **98**, 335–340.

Jones, T. D., L. A. Lebofsky, J. S. Lewis, and M. S. Marley 1990. The composition and origin of the C, P, and D asteroids: Water as a tracer of thermal evolution in the outer belt. *Icarus* **88**, 172–192.

Kessler, M. F., and 10 colleagues 1996. The Infrared Space Observatory (ISO) mission. *Astron. Astrophys.* **315**, L27–31.

Kester, D., D. Beintema, and E. Valentijn 1998. End of mission report: Wavelength calibration status. In *ISO Handbook, Vol. VI: SWS—The Short Wavelength Spectrometer.* www.iso.vilspa.esa.es/users/expl_lib.

Lagerros, J. S. V. 1996. Thermal physics of asteroids. I. Effects of shape, heat conduction, and beaming. *Astron. Astrophys.* **310**, 1011–1020.

Lagerros, J. S. V. 1997. Thermal physics of asteroids. III. Irregular shapes and albedo variegations. *Astron. Astrophys.* **325**, 1226–1236.

Lagerros, J. S. V. 1998. Thermal physics of asteroids. IV. Thermal infrared beaming. *Astron. Astrophys.* **332**, 1123–1132.

Laureijs, R. J., U. Klass, P. J. Richards, and P. Abraham 2001. Dynamical calibration. In *ISO Handbook, Vol. V: PHT—The Imaging Photo-Polarimeter.* www.iso.vilspa.esa.es/users/expl_lib.

Le Bertre, T., and B. Zellner 1980. Surface texture of Vesta from optical polarimetry. *Icarus* **43**, 172–180.

Lebofsky, L. A. 1980. Infrared reflectance spectra of asteroids—A search for water of hydration. *Astron. J.* **85**, 573–585.

Lebofsky, L. A., and J. R. Spencer 1989. Radiometry and thermal modelling of asteroids. In *Asteroids II* (R. P. Binzel, T. Gehrels, and M. S. Matthews, Eds.), p. 128. Univ. of Arizona Press, Tucson.

Lebofsky, L. A., M. V. Sykes, I. G. Nolt, J. V. Radostitz, G. J. Veeder, D. L. Matson, P. A. R. Ade, M. J. Gear, and E. I. Robson 1985. Submillimeter observations of the asteroid 10 Hygiea. *Icarus* **63**, 192–200.

Leech, K., and 27 colleagues 2000. *ISO Handbook, Vol. VI: SWS—The Short Wavelength Spectrometer*. www.iso.vilspa.esa.es/users/expl_lib.

Lemke, D., and 49 colleagues 1996. ISOPHOT—capabilities and performance. *Astron. Astrophys.* **315**, L64–70.

López-González, M. J., and E. Rodríguez 2000. Lightcurves of 10 Hygiea, 241 Germania and 509 Iolanda. *Astron. Astrophys. Supp.* **145**, 255–261.

Mennella, V., J. R. Brucato, L. Colangeli, P. Palumbo, A. Rotundi, and E. Bussoletti 1998. Temperature dependence of the absorption coefficient of cosmic analog grains in the wavelength range 20 microns to 2 millimeters. *Astrophys. J.* **496**, 1058.

Michalowski, T., F. P. Velichko, M. Lindgren, T. Oja, C.-I. Lagerkvist, and P. Magnusson 1991. The spin vector of Asteroid 10 Hygiea. *Astron. Astrophys. Supp.* **91**, 53–59.

Morris, P. 1999. SWS photometric calibrations at EOM. In *ISO Handbook, Vol. VI: SWS—The Short Wavelength Spectrometer*. www.iso.vilspa.esa.es/users/expl_lib.

Mothé–Diniz, T., M. Di Martino, P. Bendjoya, A. Doressoundiram, and F. Migliorini 2001. Rotationally resolved spectra of 10 Hygiea and a spectroscopic study of the Hygiea family. *Icarus* **152**, 117–126.

Müller, T. G., and J. S. V. Lagerros 1998. Asteroids as far-infrared photometric standards for ISOPHOT. *Astron. Astrophys.* **338**, 340–352.

Müller, T. G., J. S. V. Lagerros, M. Burgdorf, T. Lim, P. M. Morris, A. Salama, B. Schulz, and B. Vandenbussche 1999. Fundamental thermal emission parameters of main-belt asteroids derived from ISO. *ESA SP* **427**, 141.

Ragazzoni, R., A. Baruffolo, E. Marchetti, A. Ghedina, J. Farinato, and T. Niero 2000. Speckle interferometry measurements of the asteroids 10-Hygiea and 15-Eunomia. *Astron. Astrophys.* **354**, 315–320.

Rivkin, A. S. 1997. *Observations of Main-Belt Asteroids in the 3-Micron Region*. Ph.D. thesis, University of Arizona, Tucson.

Salisbury, J. W. 1993. Mid-infrared spectroscopy: Laboratory data. In *Remote Geochemical Analysis: Elemental and Mineralogical Composition* (C. M. Pieters and P. A. J. Englert, Eds.), p. 79. Cambridge Univ. Press, Cambridge.

Salisbury, J. W., D. M. D'Aria, and E. Jarosewich 1991a. Midinfrared (2.5–13.5 microns) reflectance spectra of powdered stony meteorites. *Icarus* **92**, 280–297.

Salisbury, J. W., L. S. Walter, N. Vergo, and D. M. D'Aria 1991b. Infrared (2.1–25 $\mu$m) *Spectra of Minerals*. Johns Hopkins Press, Baltimore.

Sandford, S. 1984. Infrared transmission spectra from 2.5 to 25 microns of various meteorite classes. *Icarus* **60**, 115–126.

Storrs, A., E. Wells, B. Zellner, A. Stern, and D. Durda 1999. Imaging observations of asteroids with HST. *Bull. Am. Astron. Soc.* **31**, 1103.

Tedesco, E. F., D. L. Matson, and G. J. Veeder 1989. Classification of IRAS asteroids. In *Asteroids II* (R. P. Binzel, T. Gehrels, and M. S. Matthews, Eds.), p. 290. Univ. of Arizona Press, Tucson.

Tedesco, E. F., G. J. Veeder, J. W. Fowler, and J. R. Chillemi 1992. *The IRAS Minor Planet Survey.* Phillips Laboratory, PL-TR-92-2049, Hanscon Air Force Base, MA.

Tholen, D. J. 1989. Asteroid taxonomic classifications. In *Asteroids II* (R. P. Binzel, T. Gehrels, and M. S. Matthews, Eds.), p. 1139. Univ. of Arizona Press, Tucson.

Vilas, F. 1994. A cheaper, faster, better way to detect water of hydration on Solar System bodies. *Icarus* **111**, 456–467.

Vilas, F., K. S. Jarvis, and M. J. Gaffey 1994. Iron alteration minerals in the visible and near-infrared spectra of low-albedo asteroids. *Icarus* **109**, 274–283.

Zolensky, M., and H. Y. McSween 1988. Aqueous alteration. In *Meteorites* (J. F. Kerridge, and M. S. Matthews, Eds.), p. 114. Univ. of Arizona Press, Tucson.